



Cite this: RSC Adv., 2017, 7, 8922

Received 12th December 2016  
 Accepted 23rd January 2017

DOI: 10.1039/c6ra28114a  
[rsc.li/rsc-advances](http://rsc.li/rsc-advances)

## Managing nucleophilic addition reactions to tune the physical properties of 2-substituted pentamethylBODIPY derivatives†

S. R. Sritharan,<sup>a</sup> B. A. Hussein,<sup>a</sup> D. D. Machin,<sup>a</sup> M. A. El-Aooiti,<sup>a</sup> J. A. Adjei,<sup>a</sup> J. K. Singh,<sup>a</sup> J. T. H. Pau,<sup>a</sup> J. S. Dhindsa,<sup>a</sup> A. J. Lough<sup>b</sup> and B. D. Koivisto<sup>\*a</sup>

The synthesis and characterization of a family of 2-substituted BODIPY dyes are reported herein. The dyes have been prepared using nucleophilic addition reactions (Wittig reactions, imine, Knoevenagel & aldol condensations) which are typically more challenging for BODIPY ring systems. Structure–property relationships have also been delineated by evaluating the physicochemical properties including; absorption & emission spectroscopy, electrochemical studies (CV, DPV) and theoretical calculations (TD-DFT).

## Introduction

BODIPY derivatives have received considerable attention in recent literature owing to their unique and tunable optical properties poised for a variety of applications.<sup>1–3</sup> BODIPYs, with their demiporphyrin-like structure, have been explored as biological probes,<sup>4,5</sup> photovoltaic materials,<sup>6–8</sup> photosynthetic mimics,<sup>9</sup> laser dyes<sup>10</sup> and as promising candidates for photodynamic therapy.<sup>11</sup> As such the ability to tune the optical properties (both absorbance and fluorescence) of these dyes is particularly significant depending on the nature of the desired application. Despite BODIPYs being stable in a wide range of environments (including physiological conditions), their ability to withstand classical chemical transformations is not trivial owing to their; (1) low energy LUMO orbitals which makes the  $\pi$ -system of the dipyrromethane core susceptible to nucleophilic attack, and (2) the hard acidic nature of the boron centre can readily react with hard bases like hydroxide, and alkoxides. Combined,

these behaviours can lead to decomposition and less desirable byproducts.

Owing to intense and distinct  $\pi-\pi^*$  optical transitions another significant challenge with BODIPYs is broadening and red-shifting the absorption profile for the desired application. Among others, Ziessel and co-workers have exploited the 3,5 positions of BODIPY to successfully red-shift the absorption profile.<sup>12</sup> While these type of symmetric modifications are suitable for applications involving absorption/fluorescence, they do not permit effective energy extraction because these dyes lack a suitable symmetry-breaking condition required for photo-induced charge redistribution. As such, we sought to develop a suitable and general process where one could advantageously use nucleophilic substitution reactions to electronically desymmetrize the BODIPY core for any desired application. To this end, we prepared derivatives based on the less studied pentamethylBODIPY (Fig. 1); these methylated derivatives are more stable to nucleophilic attack than unsubstituted BODIPYs and have a smaller hydrodynamic volume than BODIPYs substituted at the *meso*-position (a desired feature when considering biological applications). Furthermore, we hypothesized that having access to the readily modifiable 2,6-positions could permit greater charge separation in the excited state and allow us to effectively control the absorption spectrum of these dyes. Herein, we describe a general protocol for the preparation of a family of asymmetrically substituted BODIPYs and the structure–property relationships as a result of their varied derivatization.

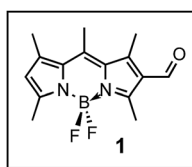


Fig. 1 PentamethylBODIPY and formylBODIPY, 1.

<sup>a</sup>Department of Chemistry and Biology, Ryerson University, 350 Victoria St. Toronto ON, M5B2K3, Canada. E-mail: bryan.koivisto@ryerson.ca

<sup>b</sup>Department of Chemistry, University of Toronto, Toronto ON, M5S 3H6, Canada

† Electronic supplementary information (ESI) available. CCDC 1522318 and 1522319. For ESI and crystallographic data in CIF or other electronic format see DOI: 10.1039/c6ra28114a

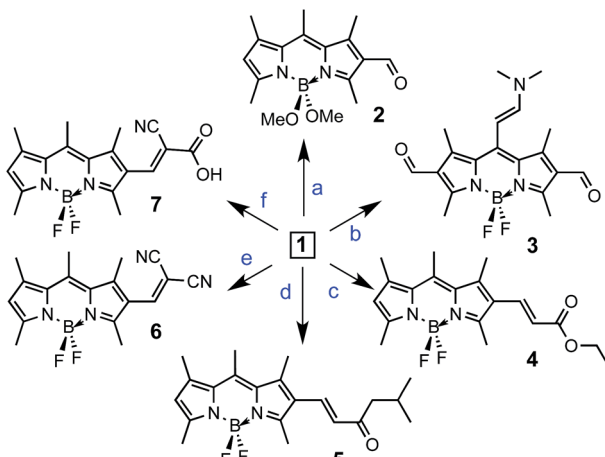
## Synthesis and characterization

Showcasing the variety of nucleophilic addition reactions possible, a number of derivatives were prepared starting with **1** (Fig. 1). FormylBODIPY, **1** has been a popular building block in



our group and its efficient synthesis has been trivialized (see ESI†) and optimized for study in the undergraduate laboratory. Scheme 1 highlights a selection of nucleophilic transformations possible. The first example in this subset, is actually a nucleophilic substitution where the fluorines have been replaced with methoxy moieties to yield derivative 2. The second example is another misfit in the set, where an attempt to further formylate **1** (using Vilsmeier–Haack conditions) actually resulted in a rather peculiar product, **3**, that was eventually identified using X-ray crystallography (Fig. 2). Evidence for similar *meso* condensations have been previously reported, and in that report product formation was surmised to be a strain driven process.<sup>13</sup> However, in our case we surmise that the significantly lower  $pK_a$  (owing to resonance stabilization) of the *meso* position permitted a Knoevenagel-like condensation with the Vilsmeier reagent (see proposed mechanism in the ESI†).

Scheme 1 also depicts the successful nucleophilic addition reactions to install conjugated carbonyl derivatives *via* Wittig (**4**), aldol (**5**) and Knoevenagel condensations<sup>14</sup> (**6** & **7**). The



**Scheme 1** Synthetic routes of BODIPY derivatives (**2–7**) from formylBODIPY (**1**): (a)  $\text{AlCl}_3$ ,  $\text{DCM}$ , reflux, 5 min, 67%; (b)  $\text{DMF}$ ,  $\text{POCl}_3$ , 57%; (c) (carboxymethylene)triphenylphosphorane, dry  $\text{DCM}$ , 12 h, rt, 50%; (d)  $\text{EtOH}$ , acetone,  $p\text{-TsOH}$  (cat.),  $\text{MgSO}_4$ , reflux, 80 °C, 24 h, 16%; (e) malononitrile,  $\text{NEt}_3$ ,  $\text{CHCl}_3$ , reflux, 16 h, 86%; (f) cyanoacetic acid,  $\text{CHCl}_3$ , piperidine, reflux, 12 h, 45%.

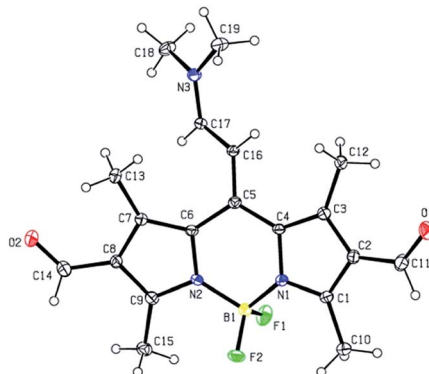


**Fig. 2** X-ray crystal structure of BODIPY derivative **3**.

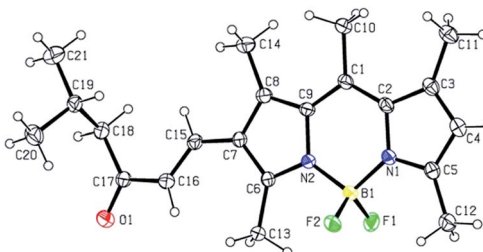
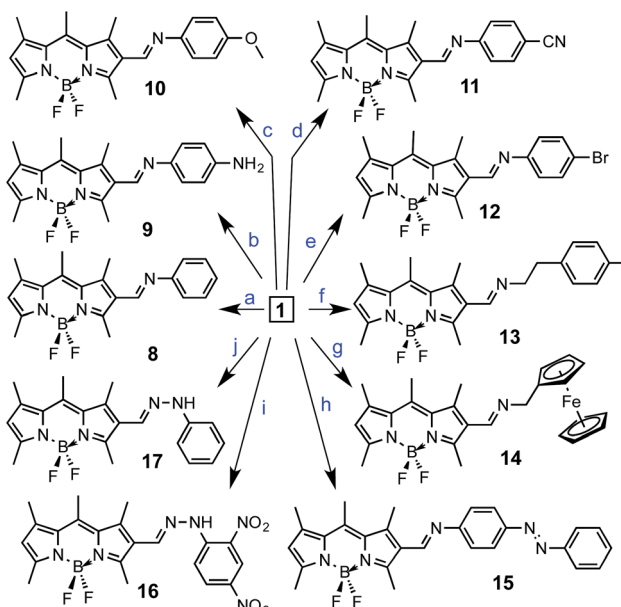


**Fig. 3** X-ray crystal structure of BODIPY derivative **5**.

Wittig reaction went smoothly so long as a stabilized phosphonium ylide was prepared and isolated in advance. Product **5** was not planned and remained a puzzling curiosity until it was identified using X-ray crystallography (Fig. 3). An aldol condensation with small (but significant) amounts of acetone led to product **5**. Finally, strong electron withdrawing groups can also be installed using Knoevenagel condensations to yield **6** and **7**.

Scheme 2 highlights the derivatization of **1**, into a variety of Schiff-bases<sup>15</sup> (**8–15**) and hydrazones (**16** & **17**) using nucleophilic addition reactions.

Within the Schiff-base family of BODIPY dyes, the intent was to explore the effect of adding electron donating or withdrawing groups in order to tune the optical properties of the dye (**8–11**).



**Scheme 2** Synthetic routes of BODIPY derivatives (**8–17**) from formylBODIPY (**1**): (a) aniline,  $p\text{-TsOH}$  (cat.),  $\text{MgSO}_4$ ,  $\text{EtOH}$ , reflux, 4 h, 15%; (b)  $p\text{-phenylenediamine}$ ,  $p\text{-TsOH}$  (cat.),  $\text{MgSO}_4$ ,  $\text{EtOH}$ , reflux, 6 h, 40%; (c)  $p\text{-anisidine}$ ,  $p\text{-TsOH}$  (cat.),  $\text{Na}_2\text{SO}_4$ ,  $\text{EtOH}$ , reflux, 1 h, 22%; (d) molecular sieves, toluene,  $4\text{-aminobenzonitrile}$ , 4.5 h, 110 °C, 73%; (e) 4-bromoaniline, dry toluene, 4 h, 110 °C, 26%; (f) 2-(*p*-tolyl)ethylamine,  $p\text{-TsOH}$  (cat.),  $\text{Na}_2\text{SO}_4$ ,  $\text{EtOH}$ , reflux, 1 h, 54%; (g) amino-methylferrocene,  $p\text{-TsOH}$  (cat.),  $\text{Na}_2\text{SO}_4$ ,  $\text{EtOH}$ , 60 h, 49%; (h) (*E*)-4-(phenyldiazenyl)aniline,  $\text{MgSO}_4$ ,  $\text{EtOH}$ , reflux 24 h, 19%; (i) 2,4-dinitrophenylhydrazine,  $\text{DCM}$ , 15 min, 61%; (j) phenylhydrazine,  $\text{DCM}$ , 2 h, rt, 54%.



Similarly, the bromide (**12**) was prepared to showcase the possibility of further modification using Pd-catalyzed cross coupling. Imine (**13**) was prepared to assess the impact of breaking conjugation with the BODIPY core, while **14** & **15** sought to marry the unique properties of ferrocene and azo-compounds with the BODIPY core, respectively. Depending on the electronic nature of the amine, the synthesis required slightly different conditions. In our hands, electron donating amines reacted smoothly, while less electron donating groups required more strenuous conditions in order to shift the equilibrium towards the imine. As a result, these reactions typically resulted in lower yields (owing to BODIPY decomposition) and disappointingly, only a minimal amount of imine **11** was isolated. It should be noted that these Schiff-bases seem to be stable in the solid state, but do hydrolyse easily under weakly acidic conditions in solution.

## Results and discussion

The physicochemical properties for compounds **1–17** (in DCM solutions), have been compared and contrasted in Table 1 and Fig. 4–8. BODIPY derivatives typically show rich electrochemical behaviour in addition to their unique optical properties. When comparing the effect of the strong electron-withdrawing groups on the physicochemical properties, malononitrile is expected to be a significantly stronger electron withdrawing group, when compared to enone **4** and aldehyde **1** (Table 1). This is seen in the observation that the oxidation of **6** occurs closer to the

Table 1 Physicochemical characterization of BODIPY (**1**) and its derivatives (**2–17**)

BODIPY dye	$E_{1/2}^a$ (V vs. NHE) $E_{ox}$	$\lambda_{max}$ emission <sup>b</sup> (nm)	UV-Vis <sup>c</sup> $\lambda_{max}$ nm ( $\epsilon \times 10^{-4}$ M <sup>-1</sup> cm <sup>-1</sup> )	Dominant FMO transition from TD-DFT
<b>1</b>	0.81	508	497(8.3)	HOMO to LUMO
<b>2</b>	0.68	—	494(2.7)	HOMO to LUMO
<b>3</b>	0.85	—	475(5.4)	HOMO to LUMO
<b>4</b>	0.79	540	521(5.5)	HOMO to LUMO
<b>5</b>	0.74	—	522(5.7)	HOMO to LUMO
<b>6</b>	0.89	—	511(2.3)	HOMO to LUMO
<b>7</b>	— <sup>d</sup>	534	513(3.8)	HOMO to LUMO
<b>8</b>	0.77	—	515(5.7)	HOMO–1 to LUMO
<b>9</b>	0.26	—	522(5.5)	HOMO–1 to LUMO
<b>10</b>	0.77	—	520(6.1)	HOMO–1 to LUMO
<b>11</b>	0.78	—	514(0.5)	HOMO to LUMO
<b>12</b>	0.78	—	517(0.9)	HOMO to LUMO
<b>13</b>	0.74	526	511(0.5)	HOMO to LUMO
<b>14</b>	0.00	579	511(3.5)	HOMO to LUMO
<b>15</b>	0.78	—	518(6.6)	HOMO–2 to LUMO
<b>16</b>	— <sup>e</sup>	—	545(0.6)	HOMO to LUMO–1
<b>17</b>	1.03	—	498(3.4)	HOMO–1 to LUMO

<sup>a</sup> Data collected using 0.1 M NBu<sub>4</sub>PF<sub>6</sub> DCM solutions at 100 mV s<sup>−1</sup> and referenced to a [Fc]/[Fc]<sup>+</sup> internal standard followed by conversion to NHE; [Fc]/[Fc]<sup>+</sup> = +765 mV vs. NHE in DCM. <sup>b</sup> Emission in DCM solutions corresponding to excitation at absorption maxima. <sup>c</sup> Low energy visible transitions from UV-Vis in DCM. <sup>d</sup> No discernible oxidation in DCM. <sup>e</sup> Insoluble in DCM.

solvent decomposition window, while the oxidation potential of **1** rests approximately 80 mV below **6**. When comparing the effect of electron withdrawing groups on the optical properties, red-shifting of the absorption profile is observed for both derivatives **4** and **6** by 24 and 14 nm, respectively, compared to the formylBODIPY **1** (Fig. 4). This is not surprising considering the TD-DFT calculations, where the dominant transitions (denoted by the solid arrow) remain the same for enone **4** and malononitrile **6**; however, the electron density shifts more towards the BODIPY core when comparing the HOMO–1 to LUMO transition. While the optical properties of formylBODIPY, **1**, are different from **4** and **6**, the electron withdrawing nature of the enone **4** and malononitrile **6** are only modestly different from each other.

When exploring the effect of varying the electronic nature of the Schiff-base, little change is observed in both the optical and electronic properties when varying the *para*-substitution. While this *para*-substituent seems to have a significant effect on the reactivity in making the derivative, comparing the effect of electron donating and withdrawing groups attached to the BODIPY they are nearly at parity when considering oxidation

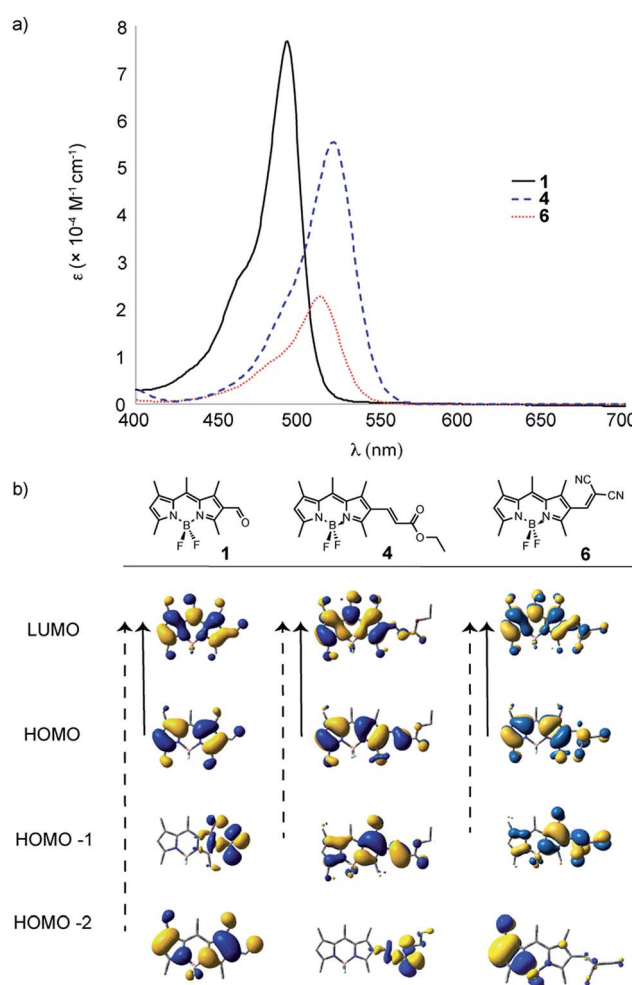


Fig. 4 UV-Vis spectra (in DCM) for target molecules **1**, **4** and **6**; comparing the effect of electronic withdrawing character after nucleophilic addition reactions with formylBODIPY **1**.



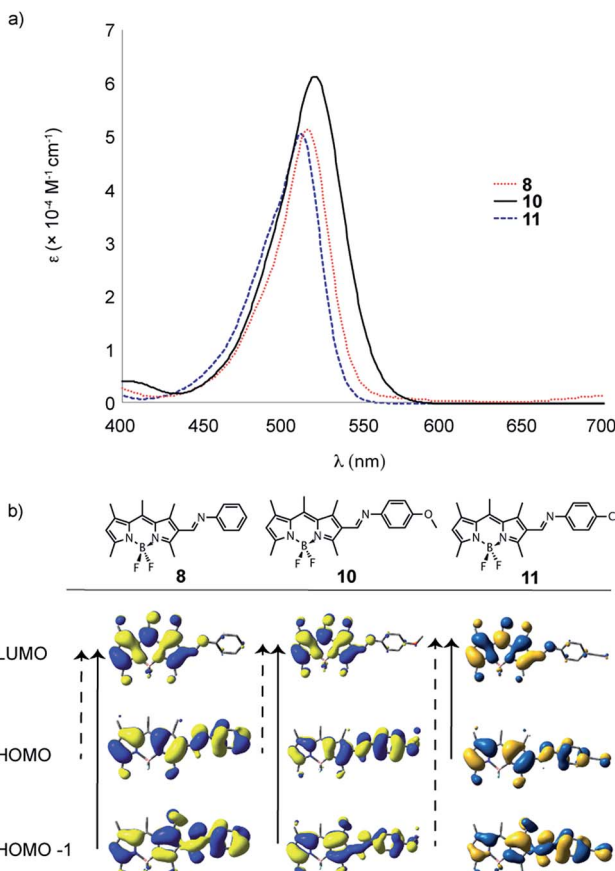


Fig. 5 UV-Vis spectra (in DCM) for target molecules **8**, **10** and **11**; comparing the effect of Schiff-base formation on a family of BODIPY dyes.

potential. Moreover, only a modest red-shift in the absorption profile is observed for **10** and a slight blue-shift is observed in the absorption profile of **11**, consistent with perturbation of the frontier orbitals (Fig. 5). When comparing the TD-DFT calculations, the dominant transitions (denoted by the dashed arrow) differ throughout the series.

When comparing the effect of extended *versus* broken conjugation in Schiff-base BODIPY derivatives **8** and **13**, a modest hypsochromic shift in the absorption profile is observed for **13** (Fig. 6); however, when a redox active substituent (ferrocene, **14**) is added a new charge transfer band emerges, despite a lack of conjugation. This is consistent with electrochemistry and DFT showing that the HOMO resides on the ferrocene portion of the molecule. Interestingly, this thermally induced charge transfer band leads to instability in dye **14**, and these ferrocene derivatives do not persist for significant periods of time in solution.<sup>16–18</sup> This has opened an entire secondary research theme in our group and we are currently examining this phenomenon in further detail (and will be the focus of a future report).

When aldehyde **1** is appended with azo-imine or hydrazone derivatives (**15**, **16**, and **17** respectively, Fig. 7 and S3†), more substantial changes to the absorption properties are observed. When comparing the optical properties of the Schiff-base

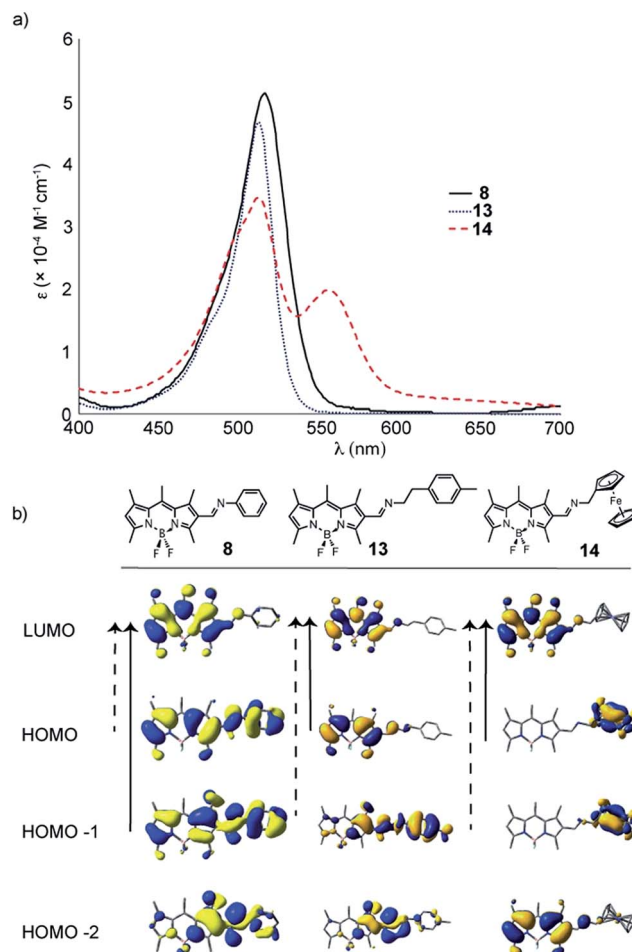


Fig. 6 UV-Vis spectra (in DCM) for target molecules **8**, **13** and **14**; comparing the effect of extended/broken conjugation in Schiff-base – base BODIPY dyes.

BODIPY derivatives, red-shifting of the absorption profile is observed for **15** by 21 nm and **16** by 21 and 48 nm, respectively, compared to the formylBODIPY **1** (Fig. 6), but poor solubility of **16** in DCM (or anything!) leads to anomalous extinction coefficients. It should be noted that the hydrazones have broad absorptions (tailing out beyond 600 nm). Based on the TD-DFT calculations, and owing to the structural diversity, the dominant transitions (denoted by the dashed arrow) differ throughout the series. When comparing the electrochemical properties, oxidation potentials are also varied and a second oxidation corresponding to the N=N bond is observed for **15** (not listed in table). As a side note, the hydrazones seem to be more stable to hydrolysis than their imine counterparts, which may suggest this is a more desirable route to alter the physical properties of BODIPY.

Finally, most of the derivatives prepared in this paper are not fluorescent; however, Fig. 8 (& Table 1) highlight some of the emissive differences in the family. Generally, the conjugated imines and hydrazones are not fluorescent, and when comparing the fluorescence of **1** & **13** (Fig. 8), there is little difference in the Stokes shift (14 & 15 nm, respectively).

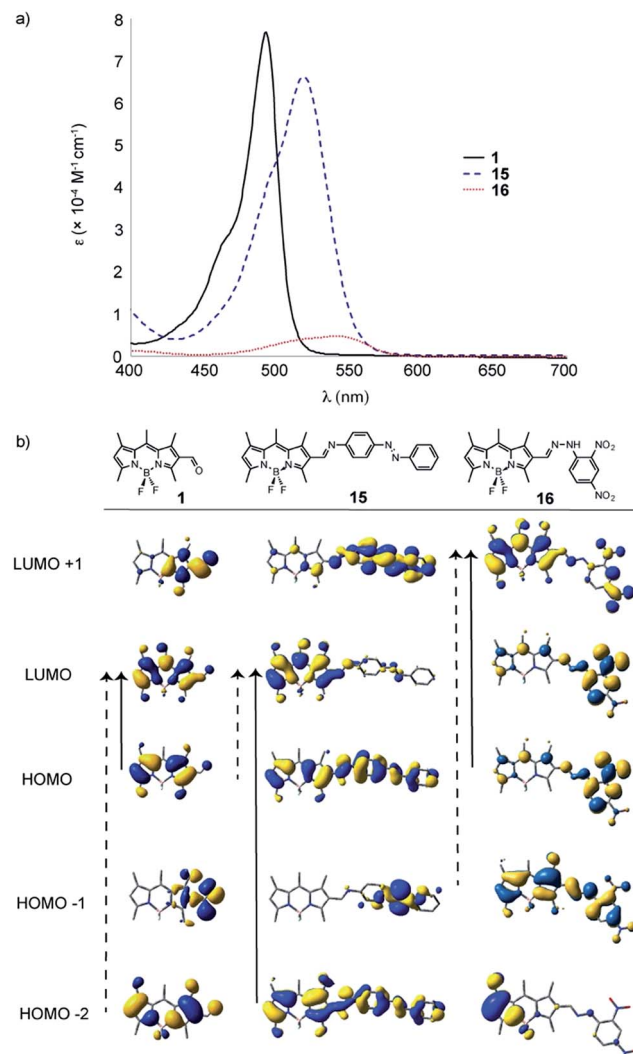


Fig. 7 UV-Vis spectra (in DCM) for target molecules **15** and **16** compared to the formylBODIPY, **1**.

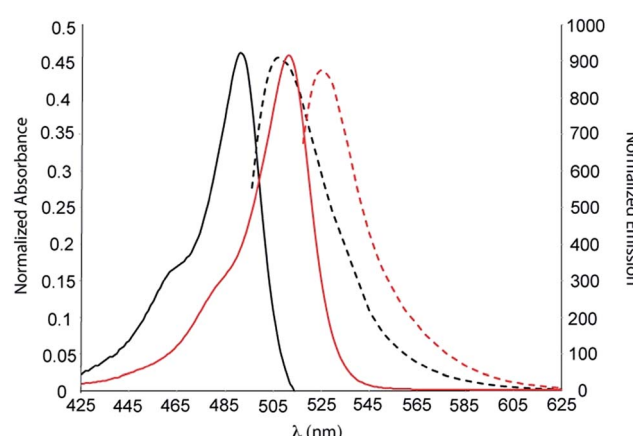


Fig. 8 UV-Vis absorption (solid lines) and normalized emission (dotted line) for molecules **1** (black) and **13** (red) (in DCM).

## Conclusions

The successful preparation of these unique, unsymmetrically-substituted derivatives suggests that despite the BODIPYs intolerance to many nucleophilic addition reactions, this current set of reactions is tolerated (although some unpredicted products do form). It also appears that functionalizing the  $\beta$ -position is an effective way to alter the physicochemical properties (and stability) of this family of dyes, with the following caveats; (a) conjugated Schiff-base modification has little effect on the physical properties, and (b) fluorescence is quenched in this Schiff-base family of molecules. The non-conjugated Schiff-base ferrocene derivative is an intriguing anomaly in this family as it readily decomposes, likely owing to the reduction of the BODIPY<sup>17</sup> and the formation of radical intermediates, although this will be elaborated on in greater detail in a forthcoming report.

## Acknowledgements

BDK would like to acknowledge NSERC and Ryerson University for financial support. In addition, BDK would like to thank former students of CHY 307/399 for their contribution in preparing building blocks necessary for this work.

## Notes and references

- 1 J. Bañuelos, *Chem. Rec.*, 2016, **16**, 335–348.
- 2 A. Bessette and G. S. Hanan, *Chem. Soc. Rev.*, 2014, **43**, 3342–3405.
- 3 A. Loudet and K. Burgess, *Chem. Rev.*, 2007, **107**, 4891–4932.
- 4 M. J. Ouairy, M. J. Ferraz, R. G. Boot and M. P. Baggelaar, *Chem. Commun.*, 2015, **51**, 6161–6163.
- 5 D. P. Murale, S. C. Hong, J. Yun, C. N. Yoon and J.-s. Lee, *Chem. Commun.*, 2015, **51**, 6643–6646.
- 6 M. Mao and Q.-H. Song, *Chem. Rec.*, 2016, **16**, 719–733.
- 7 M. Mao, X. L. Zhang, X. Q. Fang, G. H. Wu, Y. Ding, X. L. Liu, S. Y. Dai and Q. H. Song, *Org. Electron.*, 2014, **15**, 2079–2090.
- 8 C. Bonnier, D. D. Machin, O. Abdi and B. D. Koivisto, *Org. Biomol. Chem.*, 2013, **11**, 3756–3760.
- 9 M. Yousaf, A. J. Lough, E. Schott and B. D. Koivisto, *RSC Adv.*, 2015, **5**, 57490–57492.
- 10 Y. Ni and J. Wu, *Org. Biomol. Chem.*, 2014, **12**, 3774–3791.
- 11 A. Kamkaew, S. H. Lim, H. B. Lee, L. V. Kiew, L. Y. Chung and K. Burgess, *Chem. Soc. Rev.*, 2013, **42**, 77–88.
- 12 G. Ulrich, R. Ziessl and A. Harriman, *Angew. Chem., Int. Ed.*, 2008, **47**, 1184–1201.
- 13 N. Shivran, S. Mula, T. K. Ghanty and S. Chattopadhyay, *Org. Lett.*, 2011, **13**, 5870–5873.
- 14 S. Zhu, J. Zhang, G. Vegeasna, A. Tiwari, F.-T. Luo, M. Zeller, R. Luck, H. Li, S. Green and H. Liu, *RSC Adv.*, 2012, **2**, 404–407.
- 15 Y. Jia and J. Li, *Chem. Rev.*, 2015, **115**, 1597–1621.
- 16 Y. V. Zatsikha, E. Maligaspe, A. A. Purchel, N. O. Didukh, Y. F. Wang, Y. P. Kovtun, D. A. Blank and V. N. Nemykin, *Inorg. Chem.*, 2015, **54**, 7915–7928.
- 17 B. Verbelen, S. Boodts, J. Hofkens, N. I. Boens and W. Dehaen, *Angew. Chem., Int. Ed.*, 2015, **54**, 4612–4616.
- 18 S. M. Chen, W. Chen, W. Shi and H. M. Ma, *Chem.-Eur. J.*, 2012, **18**, 925–930.